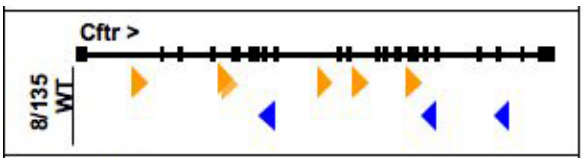

Supp. Figure 1. Orientation of SB insertions in mouse Cftr gene. Analysis of *Sleeping Beauty* transposon insertions in a screen conducted in *Apc* wildtype mice (Starr *et al*., Science, 2009) by next generation sequencing found intragenic *Cftr* insertions in 8/135 tumors. The orientation of insertions in both the forward and reverse direction is consistent with a model of gene inactivation.

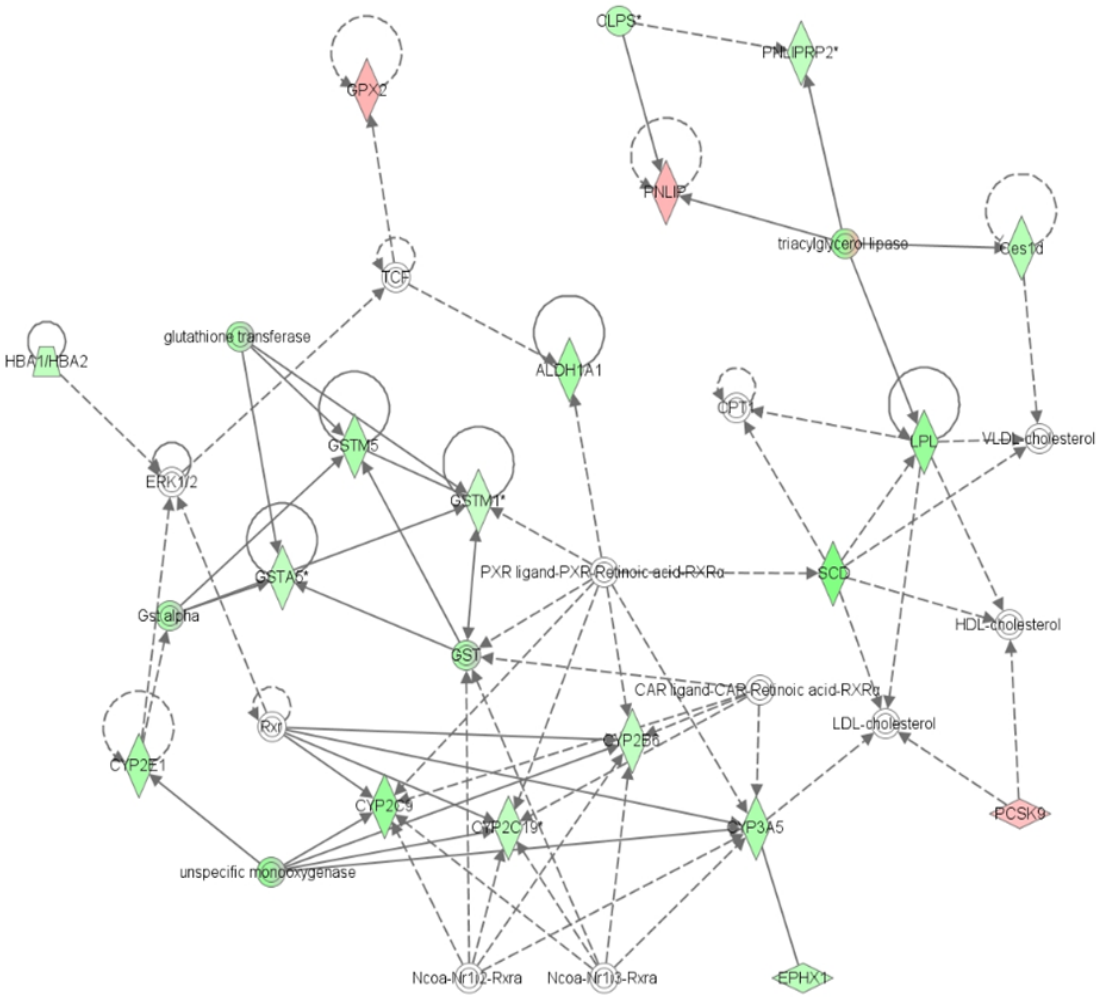

Supp Fig. 2A. Small intestine. IPA- Drug Metabolism, Small Molecule Biochemistry and Lipid Metabolism

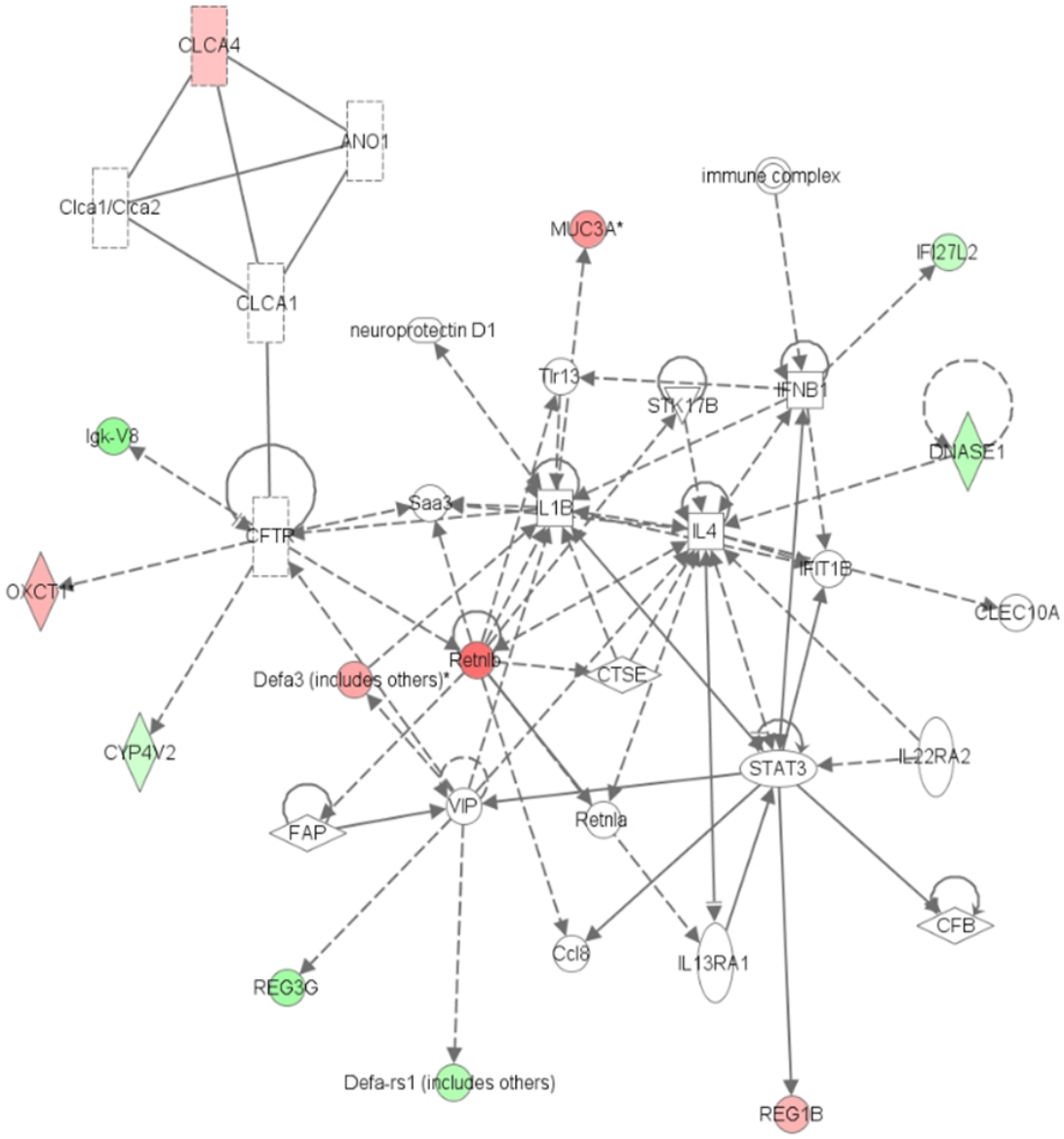

Supp. Fig. 2B. Small Intestine. IPA- Molecular Transport, Gastrointestinal Disease and Inflammatory Disease

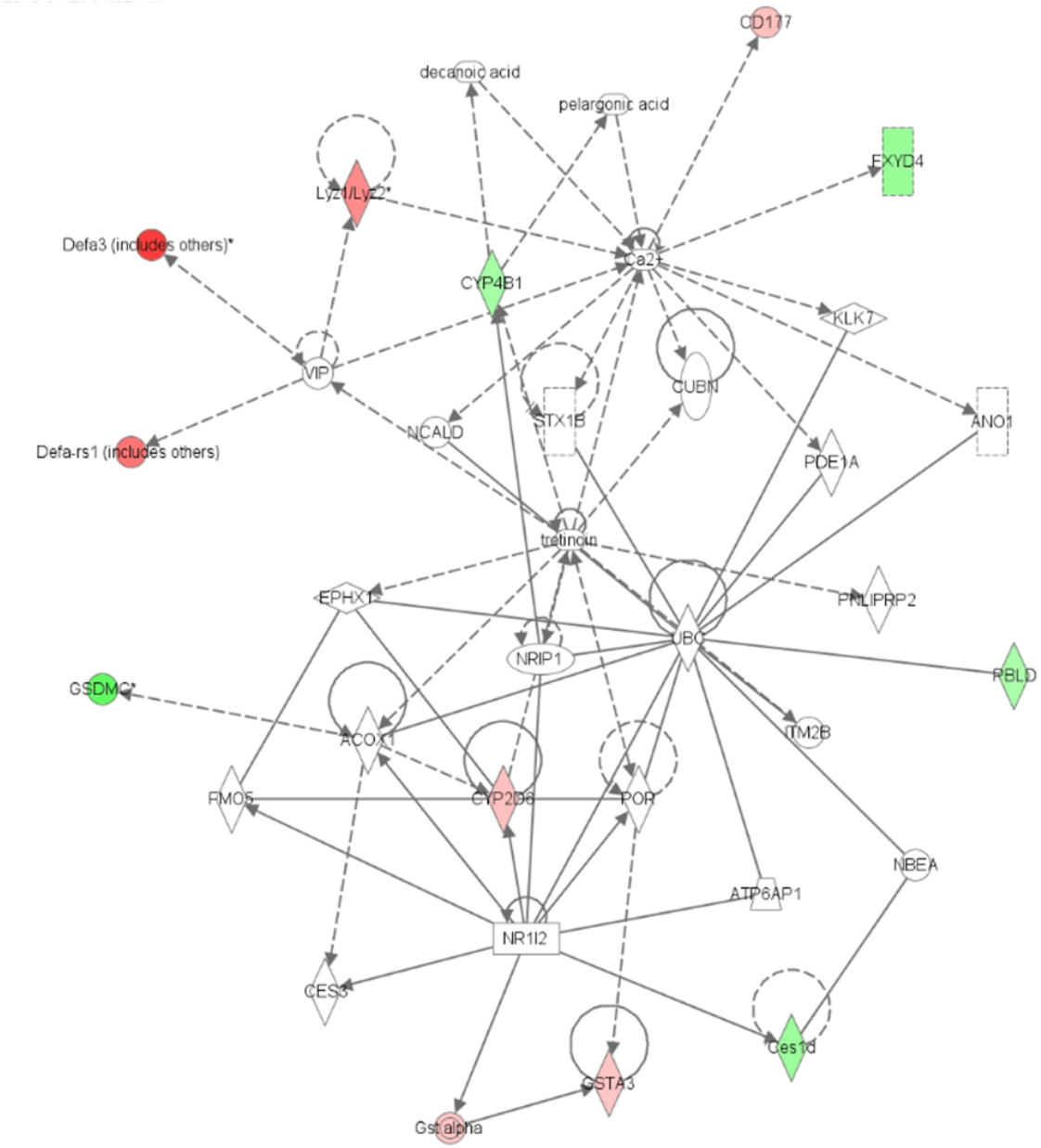

Supp. Fig. 2C. Colon. IPA- Molecular Transport, Lipid Metabolism and Small Molecule Biochemistry

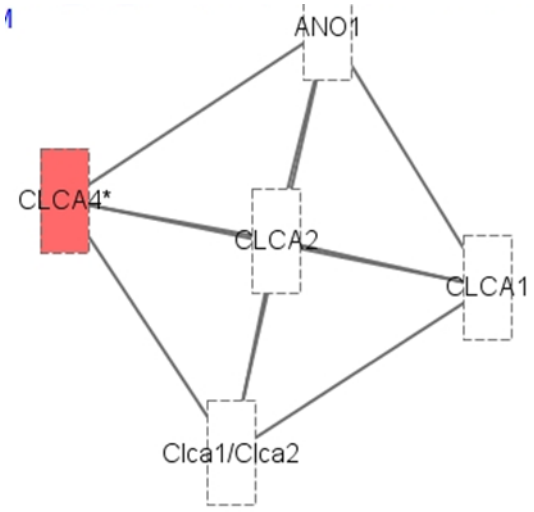

Supp. Fig. 2D. **Colon**. IPA- Cellular Growth and Proliferation, Renal and Urological System Development and Function

Supp. Fig. 3. GSEA showing enrichment plots comparing global gene expression in *Cftr*-depleted intestinal tissues to Indicated gene signatures. *Cftr*-deficient vs. *Cftr*-expressing normal epithelial-enriched intestine were compared. Gene signatures consist of (**a**) genes upregulated in *Kcnq1* KO small intestine (Than *et al*., 2014), (**b**) genes upregulated in *Kcnq1* KO colon (Than *et al*., 2014), (**c**) genes downregulated in *Muc2* small intestine (Yang *et al*., 2008). (**d**) Enrichment score (ES), normalized ES (NES), nominal p value (p) and false discovery rate q-value (FDR) are shown for each value.

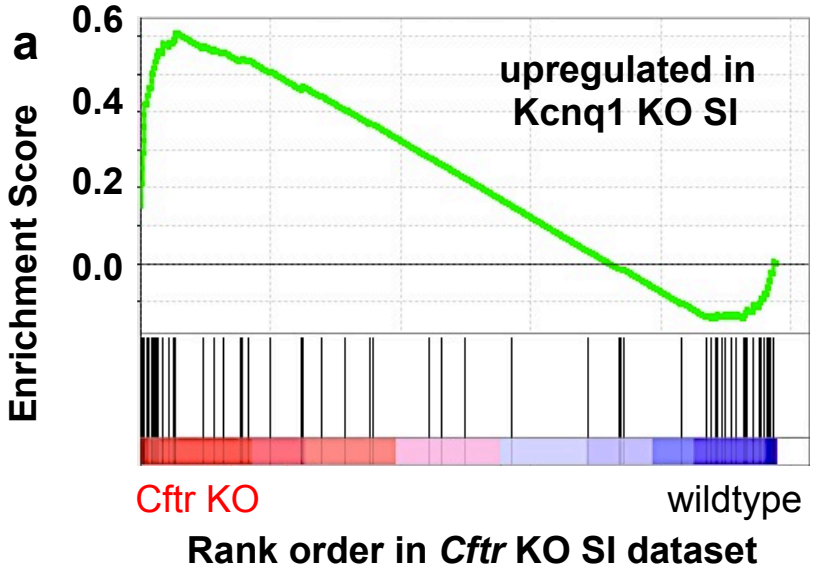

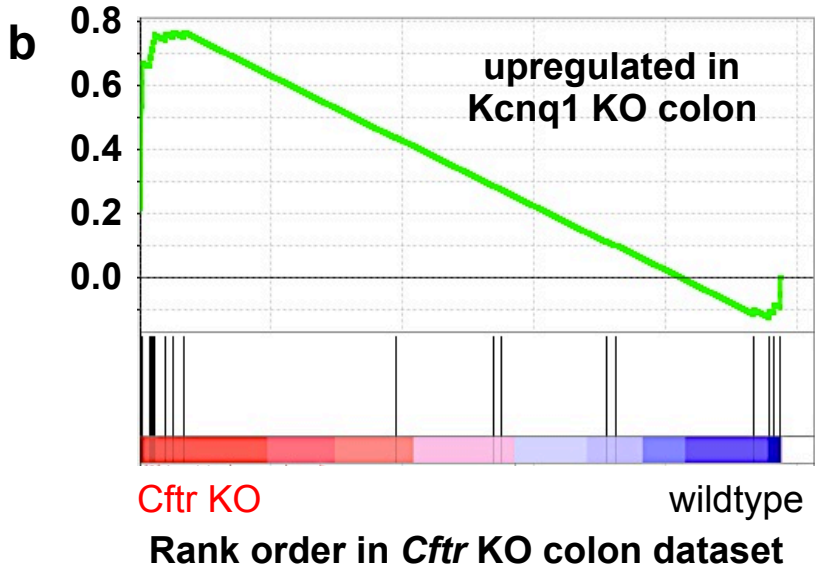

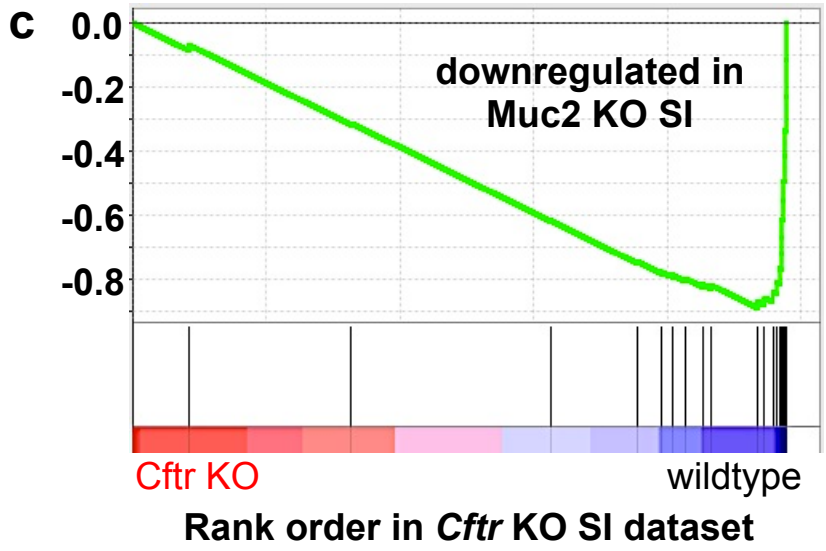

d

	vs. Cftr KO microarray			
Gene Signature	ES	NES	p	FDR
a up in Kcnq1 KO	0.61	1.88	<0.001	<0.001
b up in Kcnq1 KO	0.77	2.06	<0.001	<0.001
c down in Muc2 KO	-0.889	-2.53	<0.001	<0.001

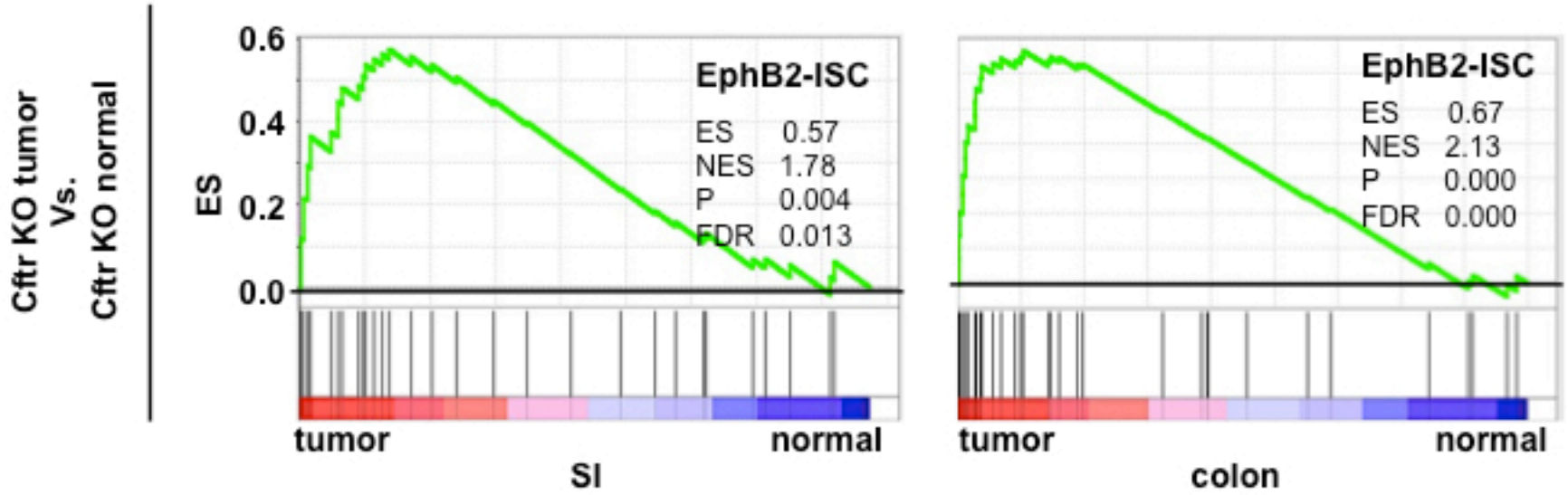

Supp. Fig. 4. GSEA showing enrichment plots comparing global gene expression in *Cftr*-depleted intestinal tissues to indicated gene signature. *Cftr*-deficient tumor vs. *Cftr*-deficient normal epithelial-enriched intestine were compared. The gene signature consists of genes upregulated in intestinal epithelial stem cells identified by EphB2^{hi} expression (*Merlos-Suarez et al., 2011*). Enrichment score (ES), normalized ES (NES), nominal p-value (p) and false discovery rate q-value (FDR) are shown for each value.

Supp. Fig. 5. **Deficiency for *Cftr* enhances colon organoid outgrowth**. 5 pairs of male littermate-matched C57Bl/6J *Cftr*$^{fl/fl}$ and *Cftr*$^{fl/fl}$ *Villin-Cre*$^{+}$ mice were sacrificed between 8 and 12 weeks of age. Colons were removed, cut open and washed in cold PBS. Colon organoids were then cultured using the protocol of Sato et al, 2011, following the plating of 500 crypt bottoms per well in triplicate per sample. * $P < 0.05$.

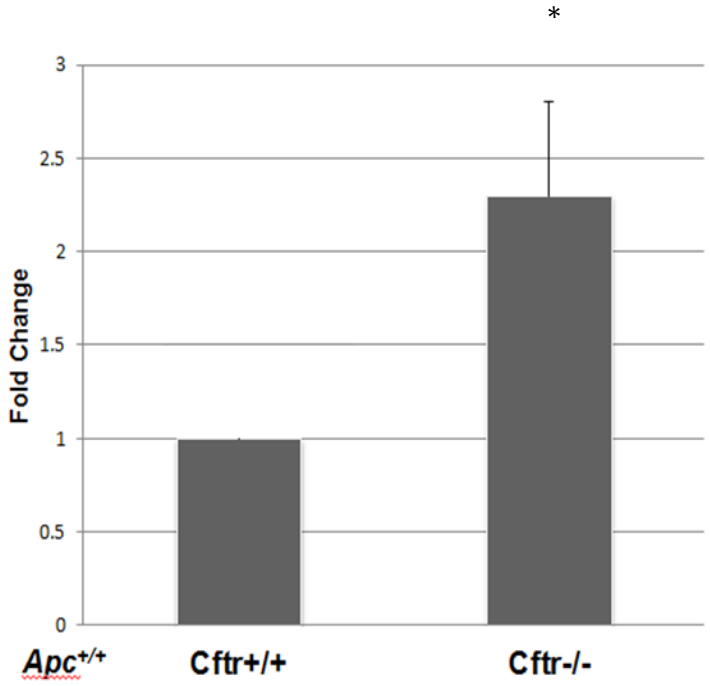

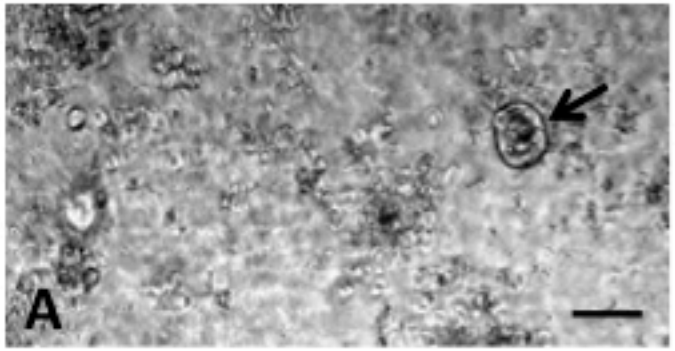

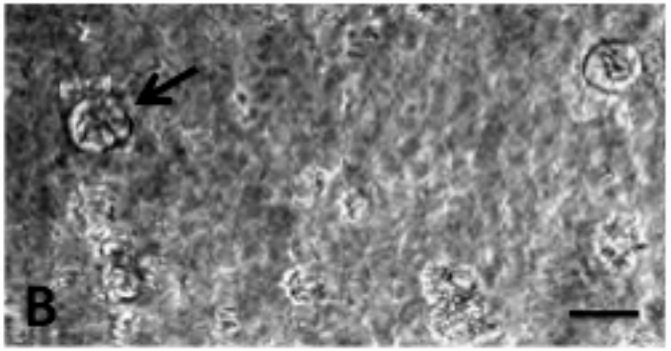

Supplemental Figure 5B. **No morphological differences between C57Bl/6J Cftr$^{fl/fl}$** (Panel A, bar = 10X) **and Cftrf$^{l/fl}$ Villin-Cre^{+}** (Panel B, bar = 10X) **colon organoids**. Examples of colon organoids are indicated by arrows in both panels.

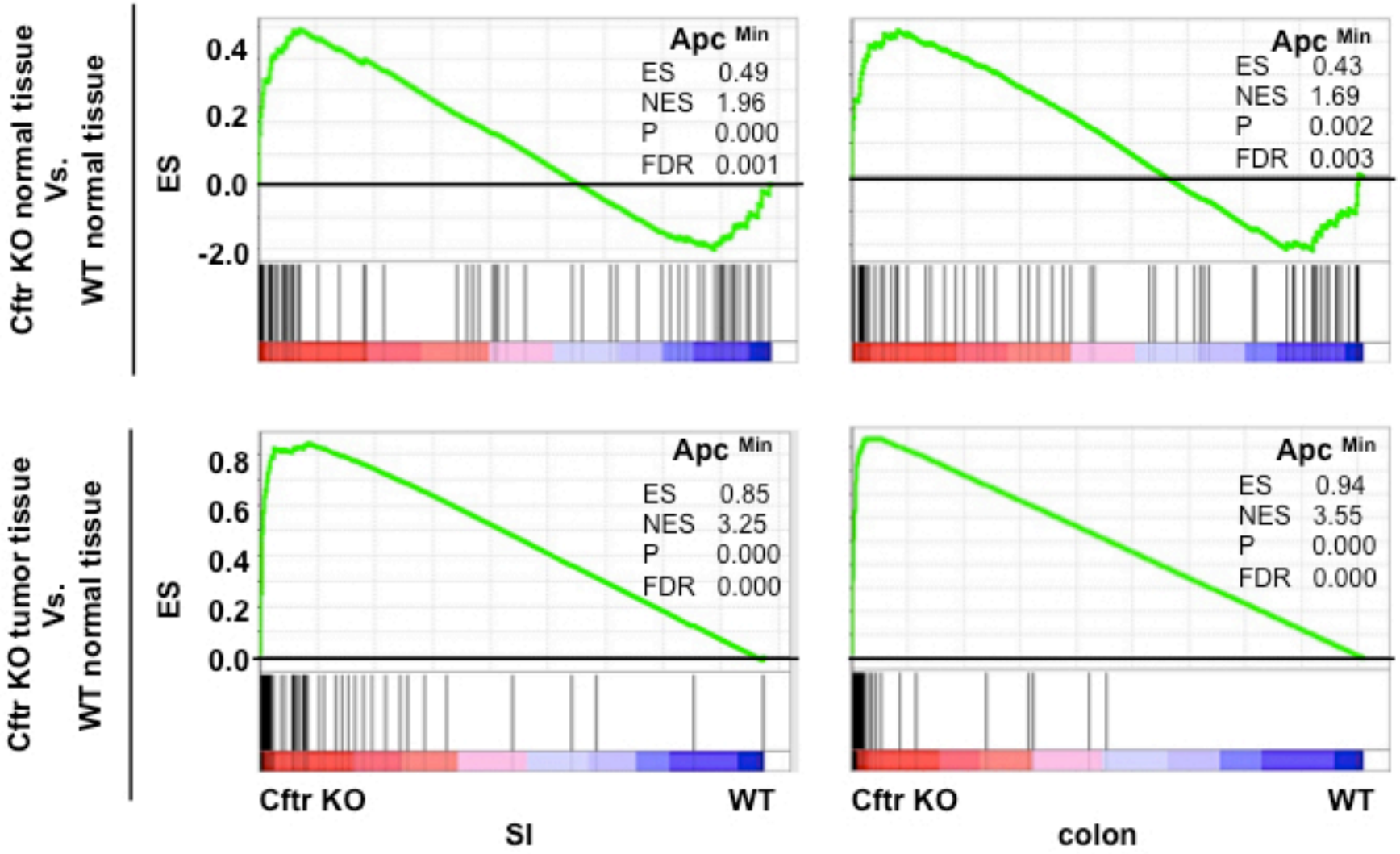

Supp. Fig. 6. GSEA showing enrichment plots comparing global gene expression in *Cftr*-depleted intestinal tissues to indicated gene signatures. *Cftr*-deficient (tumor or normal) vs. Cftr-expressing normal epithelial-enriched intestine were compared. Gene signature consists of genes upregulated in *Apc*^{Min} adenomas (SI or colon). Enrichment score (ES), normalized ES (NES), nominal p-value (p) and false discovery rate q-value (FDR) are shown for each value.

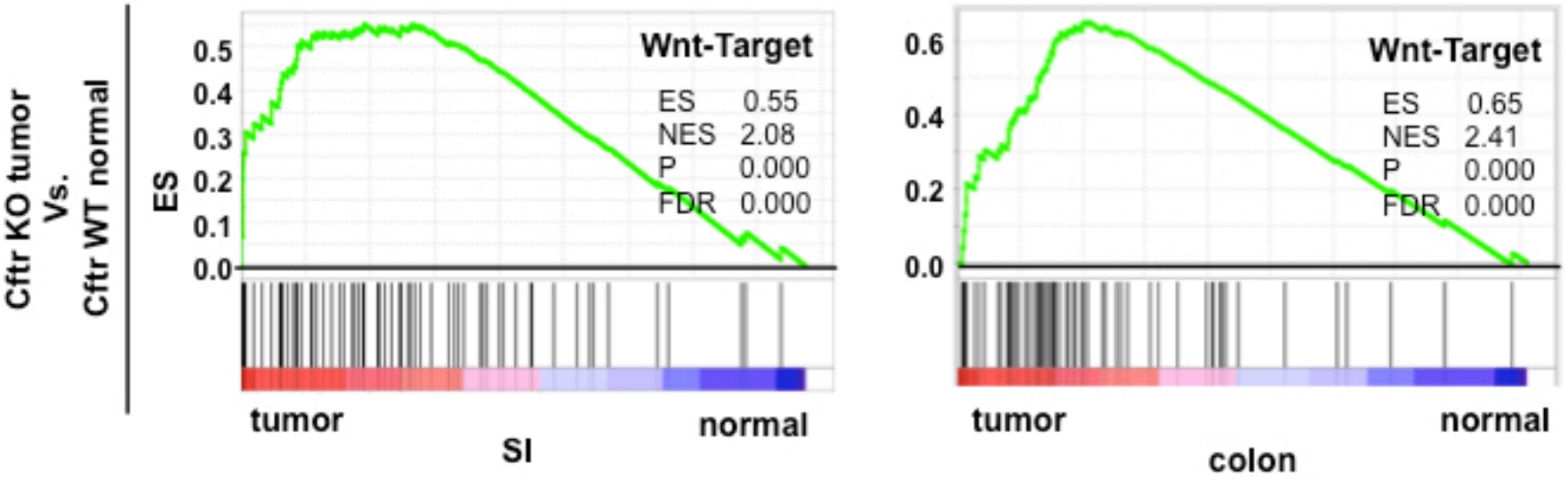

Supp. Fig. 7. GSEA showing enrichment plots comparing global gene expression in *Cftr*-depleted intestinal tissues to indicated gene signatures. *Cftr*-deficient tumors vs. Cftr-expressing normal epithelial-enriched intestine were compared. Gene signatures consist of Wnt target genes (van der Flier et al., 2007). Enrichment score (ES), normalized ES (NES), nominal p-value (p) and false discovery rate q-value (FDR) are shown for each value.

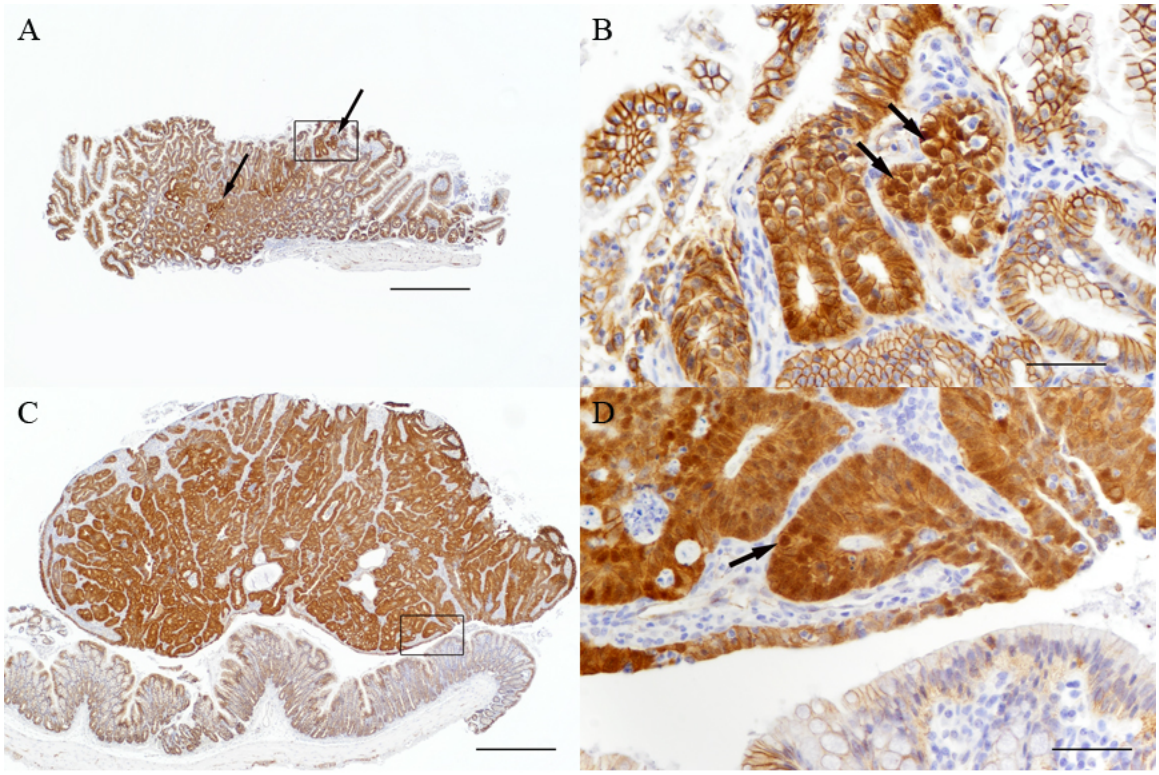

Supp. Figure 8. β-catenin immunohistochemistry.

Representative image of analysis of 4 small intestine adenomas (2 jejunum, 1 ileum, 1 duodenum) from *Apc*$^{+/+}$ *Cftr*$^{fl/fl}$*-Villin-Cre* mice and similar adenomas from *Apc*^{Min} mice.

Panel A. Small intestine adenoma from *Apc*$^{+/+}$ *Cftr*$^{fl/fl}$*-Villin-Cre* mouse showing multifocal areas with increased expression of β-catenin (arrows).
Panel B. Same adenoma as in panel A shows increased cytoplasmic labelling and nuclear translocation of β-catenin (arrows).
Panel C. Small intestine adenoma from *Apc*^{Min} mouse shows diffuse increased expression of β-catenin (arrow).
Panel D. Same adenoma as in panel C shows increased cytoplasmic labelling and nuclear translocation of β-catenin (arrow).

Panels B and D are high magnification images of the areas indicated by rectangular boxes in Panels A and C, respectively. Bars in panels A and C, and B and D are 500 and 50 µms, respectively.

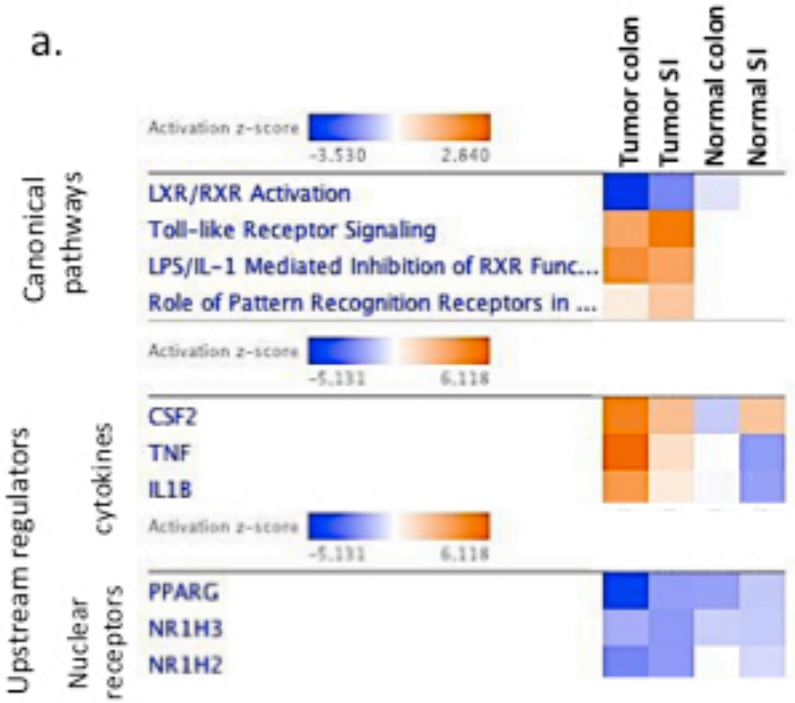

Supp. Fig. 9. IPA analysis of gene expression changes in each of four *Cftr*-deficient tissues: colon tumor, small intestine (SI) tumor, normal colon, and normal SI, to identify pathways with overlapping changes in gene expression.
a. Heatmap of z-scores indicating overlap of LXR/RXR, Toll-like receptor, related canonical pathways, and upstream regulators with gene expression changes in *Cftr*-deficient tissues. Z-score indicating extent and direction of overlap for each pathway is shown.

b. Heatmap representing expression levels of overlapping genes in LXR/RXR and Toll-like receptor pathways in each tissue is shown.

b.

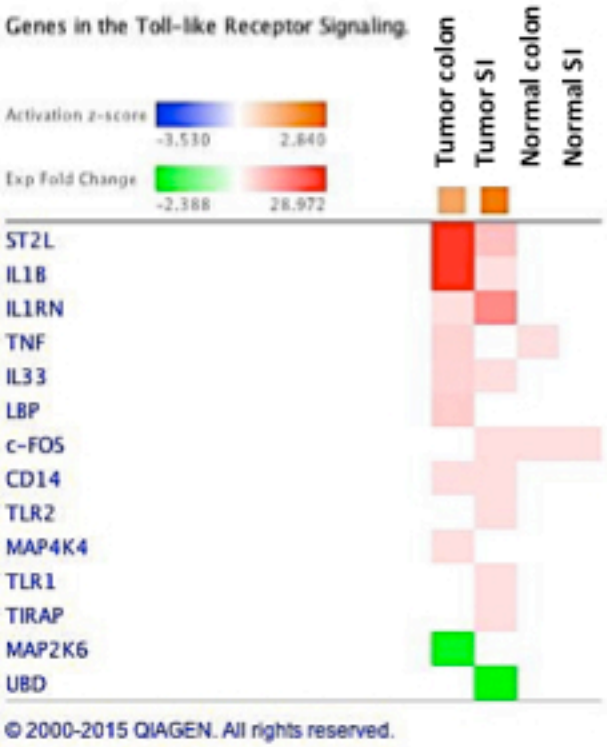
Genes in the Toll-like Receptor Signaling
Activation z-score
-3.530
2.840
Exp Fold Change
-2.388
28.972
Tumor colon
Tumor SI
Normal colon
Normal SI
ST2L
IL1B
IL1RN
TNF
IL33
LBP
c-FOS
CD14
TLR2
MAP4K4
TLR1
TIRAP
MAP2K6
UBD
© 2000-2015 QIAGEN. All rights reserved.


Genes in the LXR/RXR Activation network
Activation z-score
-3.530
2.840
Exp Fold Change
-43.201
28.972
Tumor colon
Tumor SI
Normal colon
Normal SI
IL1RL1
IL1B
TNFRSF11B
IL1RN
PTGS2
iNOS
CLU
MMP9
TNF-α
IL33
LBP
CD14
C4A/C4B
APOD
SERPINF1
C3
TNFRSF1B
SR-A
ABCG1
IL1RL2
TF
ABCG8
LYZ
APOB
ABCA1
ApoC2
CD36
AGT
MLXIPL
ABCG5
SCD1
LPL
ApoA1
ApoA4
© 2000-2015 QIAGEN. All rights reserved.

Supp. Fig. 10. Gene expression analyses based on RNA Seq data from AMC90 cohort